Supplementary Information: Deciphering Age- and Sex-Specific Patterns of Coronary Artery Atherosclerosis from a Large Chinese Cohort

Xinnian YANG[1,2,3,+], Jiayin Zhang[4,+], Yanli Song[5], Dengqiang Jia[6,3], Qingqi Hong[7], Yiqiang Zhan[5], Xiang Sean Zhou[5], Yining Dong[1], Yining Wang[8,*], Dijia Wu[5,**], Dinggang Shen[2,5,9,***]

[1]School of Data Science, City University of Hong Kong, Hong Kong, China.
[2]School of Biomedical Engineering & State Key Laboratory of Advanced Medical Materials and Devices, ShanghaiTech University, Shanghai 201210, China.
[3]Hong Kong Centre for Cerebro-cardiovascular Health Engineering, Hong Kong, China.
[4]Department of Radiology, Shanghai General Hospital, Shanghai Jiao Tong University School of Medicine, Shanghai 200080, China.
[5]Shanghai United Imaging Intelligence Co., Ltd., Shanghai 200232, China.
[6]Faculty of Applied Sciences, Macao Polytechnic University, Macao 999078, China.
[7]National Institute for Data Science in Health and Medicine, Xiamen University, Xiamen 361005, China.
[8]Department of Radiology, State Key Laboratory of Complex Severe and Rare Diseases, Peking Union Medical College Hospital, Chinese Academy of Medical Sciences and Peking Union Medical College, Beijing 100730, China.
[9]Shanghai Clinical Research and Trial Center, Shanghai 201210, China.
[*]wangyining@pumch.cn.
[**]dijia.wu@uii-ai.com.
[***]dinggang.shen@gmail.com.
[+]These authors contributed equally to this work.

Contents

List of Figures

List of Tables

1 Supplementary Results

1.1 PLASMA system operational efficiency

To assess the practical efficiency of PLASMA in clinical workflows, we systematically evaluated its computation time and memory consumption by repeatedly processing 232 CCTA cases across five different types of GPU configurations. Computation time was defined as the total time from the input of a CCTA scan to the output of all interpretation results. The mean per-patient computation time of PLASMA is 17.12±3.72 seconds at NVIDIA GeForce RTX 4060 Ti with Intel® Core™ i9-12900K), 25.25±6.16 seconds at NVIDIA RTX A4000 with Intel® Xeon® Silver 4210R and 29.95±7.31 seconds at NVIDIA RTX 2080 Ti with Intel® Xeon® Silver 4110, see more details in Supplementary Table 2. These times cover the entire automated pipeline, including coronary segmentation, plaque detection and quantification, stenosis grading, high-risk feature classification, and pre-processing operations.

For comparison, our previous study[1] reported that the mean post-processing and reading time by radiologists for anatomical and stenosis analysis, assisted by a dedicated workstation, was 186.61±99.72 seconds per case. Moreover, Lin et al.[2] demonstrated that manual plaque analysis using semi-automated research software (Autoplaque version 2.5; Cedars-Sinai Medical Center, Los Angeles, USA)[3] required 25.66±6.79 minutes per patient. These results indicate that PLASMA offers substantial improvements in operational efficiency over manual and semi-automated workflows, achieving fully automated interpretation under one minute per case, even on mid-range hardware. Meanwhile, the maximum RAM required to execute PLASMA did not exceed 6 GB, and the maximum GPU memory demand remained below 5 GB. The efficiency supports its practical deployment in real-world clinical settings.

1.2 Regional subgroup analyses of coronary atherosclerosis in China

Our study incorporated multiple centers across mainland China, covering both economically developed and underdeveloped regions, as well as seven major geographical areas. Given that economic status, lifestyle, and dietary factors may influence the CAD development in a population, two regional subgroup analyses were performed to further demonstrate the applicability of our findings: one comparing rural and urban populations, and the other examining the seven major geographical regions included in the cohort.

1.2.1 Rural vs. urban populations

As CCTA is an advanced imaging modality that is more commonly accessible in urban centers, data originating from third-tier cities[4] were classified as representing economically less-developed regions, serving as a proxy for rural settings, which constituted a minority of the cohort. The remaining data were classified as originating from well-developed, i.e., urban areas. Our cohort included $n = 14,923$ from urban areas and $n = 1,377$ from rural areas. Age and gender distributions for rural and urban populations are provided in Supplementary Table 4.

Results showed that individuals undergoing CCTA in rural regions (mean age: 58.12±11.54 years) were, on average, younger than those in urban areas (mean age: 61.80±11.65 years). Regarding overall atherosclerotic burden, the average total plaque volume was higher in rural group (mean±SD: 343.88±468.24 mm^3; median: 165.33 mm^3; IQR: 24.76–469.94 mm^3) compared to the urban group (mean±SD: 291.78±415.65 mm^3; median: 126.16 mm^3; IQR: 0.00–404.29 mm^3), whereas calcified plaque volume was lower in the rural regions. Compared to North American populations, despite slight differences in age distribution between rural, urban, and North American cohorts, the average total plaque burden in any subgroup remained lower than that observed in North America (mean±SD: 413.5±515.0 mm^3; median: 223 mm^3; IQR: 29–614 mm^3). These findings were consistent across the entire, female, and male populations.

Supplementary Figure 3 illustrates the sex differences of plaque progression and the age gap in atherosclerosis onset between rural and urban populations. Importantly, both settings showed patterns consistent with the main manuscript findings: females exhibited an approximately 20-year delayed onset of atherosclerosis relative to males, with a nonlinear increase in plaque burden with age, whereas males showed a more linear and steady increase. These consistent trends across rural and urban populations reinforce the robustness of our overall conclusions.

1.2.2 Seven major geographic regions in mainland China

The seven major geographical regions analyzed included East ($n = 3,333$), North ($n = 2,680$), Northeast ($n = 2,979$), Northwest ($n = 1,120$), Southwest ($n = 2,100$), Central ($n = 2,696$), and South ($n = 1,392$). The results are summarized in Supplementary Table 5. Across all regions, the average total plaque volume remained lower than that observed in North American population. Among these regions, the Northern population exhibited the highest overall atherosclerosis burden (mean±std: 375.45±482.78, median: 199.13, IQR: 22.49–545.53 mm^3), while the Southwestern population exhibited the lowest overall burden (mean±std: 255.27±376.37 , median: 126.38, IQR: 3.89–414.97 mm^3).

The overall pattern of delayed onset in females were preserved across all regions. Although the specific year-gap values varied across regions, the majority were consistent with an approximate 20-year delay, while the Southwestern and Southern regions exhibited longer delays, 24 and 25 years respectively. Despite numerical differences, the overall pattern of delayed onset in females remained consistent across regions, supporting the generalizability of our findings.

References

[1] Yang, W., Chen, C., Yang, Y., Chen, L., Yang, C., Gong, L., Wang, J., Shi, F., Wu, D., Yan, F.: Diagnostic performance of deep learning-based vessel extraction and stenosis detection on coronary computed tomography angiography for coronary artery disease: a multi-reader multi-case study. La radiologia medica **128**(3), 307–315 (2023)

[2] Lin, A., Manral, N., McElhinney, P., Killekar, A., Matsumoto, H., Kwiecinski, J., Pieszko, K., Razipour, A., Grodecki, K., Park, C., *et al.*: Deep learning-enabled coronary ct angiography for plaque and stenosis quantification and cardiac risk prediction: an international multicentre study. The Lancet Digital Health **4**(4), 256–265 (2022)

[3] Matsumoto, H., Watanabe, S., Kyo, E., Tsuji, T., Ando, Y., Otaki, Y., Cadet, S., Gransar, H., Berman, D.S., Slomka, P., *et al.*: Standardized volumetric plaque quantification and characterization from coronary ct angiography: a head-to-head comparison with invasive intravascular ultrasound. European radiology **29**, 6129–6139 (2019)

[4] The State Council of the People's Republic of China: Notice on Issuing the Guidelines for Promoting the High-Quality Development of Private Medical Institutions. Official Notice, The State Council of China. Available at: https://www.gov.cn/lianbo/bumen/202406/content_6957699.htm (2024)

[5] Tzimas, G., Gulsin, G.S., Everett, R.J., Akodad, M., Meier, D., Sewnarain, K., Ally, Z., Alnamasy, R., Ng, N., Mullen, S., *et al.*: Age-and sex-specific nomographic ct quantitative plaque data from a large international cohort. JACC: Cardiovascular Imaging **17**(2), 165–175 (2024)

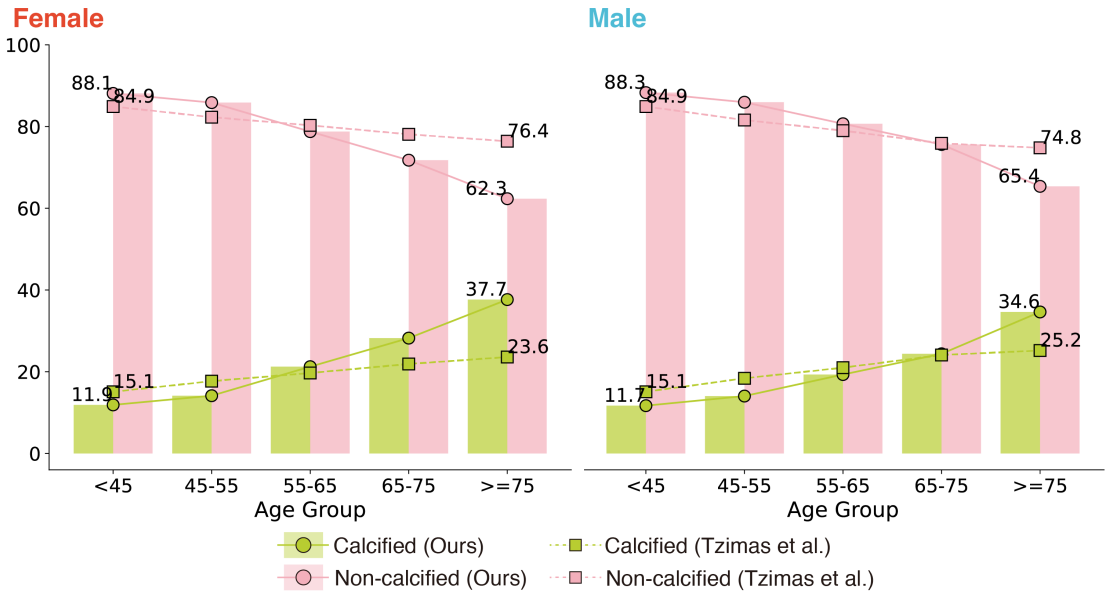

Supplementary Figure 1: **Calcified and non-calcified proportion changes stratified by sex compared with the North American population**[5]**.** Dashed lines and square points represent results from the North American population. The left panel shows female data, and the right panel shows male data.

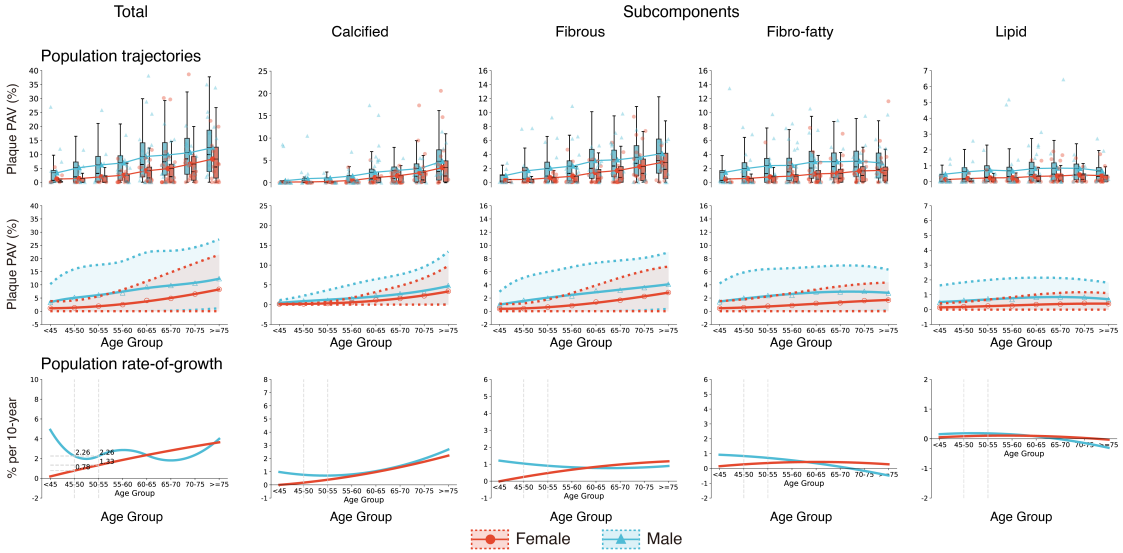

Supplementary Figure 2: **Sex differences in plaque burden characteristics under finer age stratification.** (The 1st and 2nd rows) Box plots of plaque PAV distributions across age groups, with PAV-age trajectories of mean (dotted lines indicating 10% and 90% centiles) estimated by cubic B-spline (smooth factor=0.1). (The 3rd row) Rates of PAV change over the lifespan, derived from PAV-age trajectories. All plots are stratified by sex (female, red; male, blue).

Supplementary Table 1: Performance of PLASMA versus experts plaque volume quantification in internal five-fold cross-validation setting ($n = 1,560$). Intraclass correlation coefficients (ICC) with corresponding p values and Pearson's correlation coefficients were calculated to assess agreement between PLASMA and expert measurements for total, calcified, non-calcified, and lipid plaque volumes. p values for ICC were derived from one-sided F-tests.

Plaque Type	Fold	ICC (95% CI)	p-value	Pearson's r (95% CI)
Total Plaque Volume	Fold0	0.94 (0.93–0.95)	7.98×10^{-144}	0.95 (0.93–0.96)
	Fold1	0.89 (0.86–0.91)	1.15×10^{-102}	0.90 (0.87–0.92)
	Fold2	0.89 (0.86–0.91)	2.61×10^{-102}	0.90 (0.87–0.92)
	Fold3	0.94 (0.93–0.95)	3.94×10^{-142}	0.96 (0.95–0.97)
	Fold4	0.94 (0.93–0.96)	1.49×10^{-144}	0.95 (0.94–0.96)
	avg.	**0.92 ± 0.0274**	**<0.0001**	**0.93 ± 0.0295**
Calcified Plaque Volume	Fold0	0.99 (0.98–0.99)	2.12×10^{-206}	0.99 (0.99–0.99)
	Fold1	0.98 (0.97–0.98)	2.80×10^{-175}	0.99 (0.98–0.99)
	Fold2	0.99 (0.99–0.99)	1.47×10^{-215}	1.00 (0.99–1.00)
	Fold3	0.99 (0.99–1.00)	8.59×10^{-264}	1.00 (0.99–1.00)
	Fold4	0.99 (0.99–0.99)	4.31×10^{-233}	1.00 (0.99–1.00)
	avg.	**0.99 ± 0.0045**	**<0.0001**	**1.00 ± 0.0055**
Non-calcified Plaque Volume	Fold0	0.90 (0.88–0.92)	1.74×10^{-111}	0.91 (0.89–0.93)
	Fold1	0.83 (0.79–0.87)	1.70×10^{-78}	0.84 (0.81–0.87)
	Fold2	0.85 (0.81–0.88)	5.61×10^{-83}	0.86 (0.82–0.88)
	Fold3	0.91 (0.88–0.92)	2.52×10^{-114}	0.94 (0.93–0.95)
	Fold4	0.92 (0.90–0.94)	9.14×10^{-124}	0.93 (0.91–0.94)
	avg.	**0.88 ± 0.0396**	**<0.0001**	**0.90 ± 0.0439**
Lipid Plaque Volume	Fold0	0.71 (0.65–0.77)	5.86×10^{-47}	0.77 (0.72–0.81)
	Fold1	0.59 (0.51–0.66)	3.81×10^{-29}	0.64 (0.57–0.70)
	Fold2	0.55 (0.47–0.63)	5.86×10^{-25}	0.65 (0.58–0.71)
	Fold3	0.58 (0.50–0.65)	4.50×10^{-28}	0.73 (0.67–0.78)
	Fold4	0.70 (0.63–0.75)	1.30×10^{-43}	0.79 (0.74–0.83)
	avg.	**0.63 ± 0.0737**	**<0.0001**	**0.72 ± 0.0684**

ICC = Intraclass Correlation Coefficient; CI = Confidence Interval. The avg. represent the mean ± standard deviation across folds. Higher ICC and Pearson's r values indicate better agreement.

Supplementary Table 2: Computation time and memory use of PLASMA across five GPUs. Results are based on testing with a single GPU. Mean per-case computation time was measured on 232 CCTA scans processed through the fully automated pipeline, including coronary segmentation, plaque detection and quantification, stenosis grading and high-risk feature classification.

GPU+CPU Model	Computation Time, s	RAM, GB	GPU, GB
NVIDIA GeForce RTX 4060 Ti + Intel® Core™ i9-12900K	17.12±3.72 (10.12–26.00)	3.78±0.35 (3.34–5.47)	3.99±0.21 (3.49–4.60)
NVIDIA GeForce RTX 3060 + Intel® Core™ i9-10900X	19.56±5.54 (9.87–32.46)	3.79±0.33 (3.36–5.51)	3.91±0.32 (2.81–4.68)
NVIDIA RTX A4000 + Intel® Xeon® Silver 4210R	25.25±6.16 (13.32–36.37)	3.79±0.35 (3.32–5.72)	
Quadro RTX 4000 + Intel® Xeon® Silver 4210	26.00±6.80 (14.61–41.37)	2.76±0.36 (2.32–4.79)	
NVIDIA GeForce RTX 2080 Ti + Intel® Xeon® Silver 4110	29.95±7.31 (16.71–45.96)	2.77±0.34 (2.31–4.59)	

Values are presented as mean±standard deviation (SD) and range (minimum–maximum) for computation time, RAM usage, and GPU memory usage. The reported RAM consumption reflects the parallel resource requirements during GPU-accelerated computations.

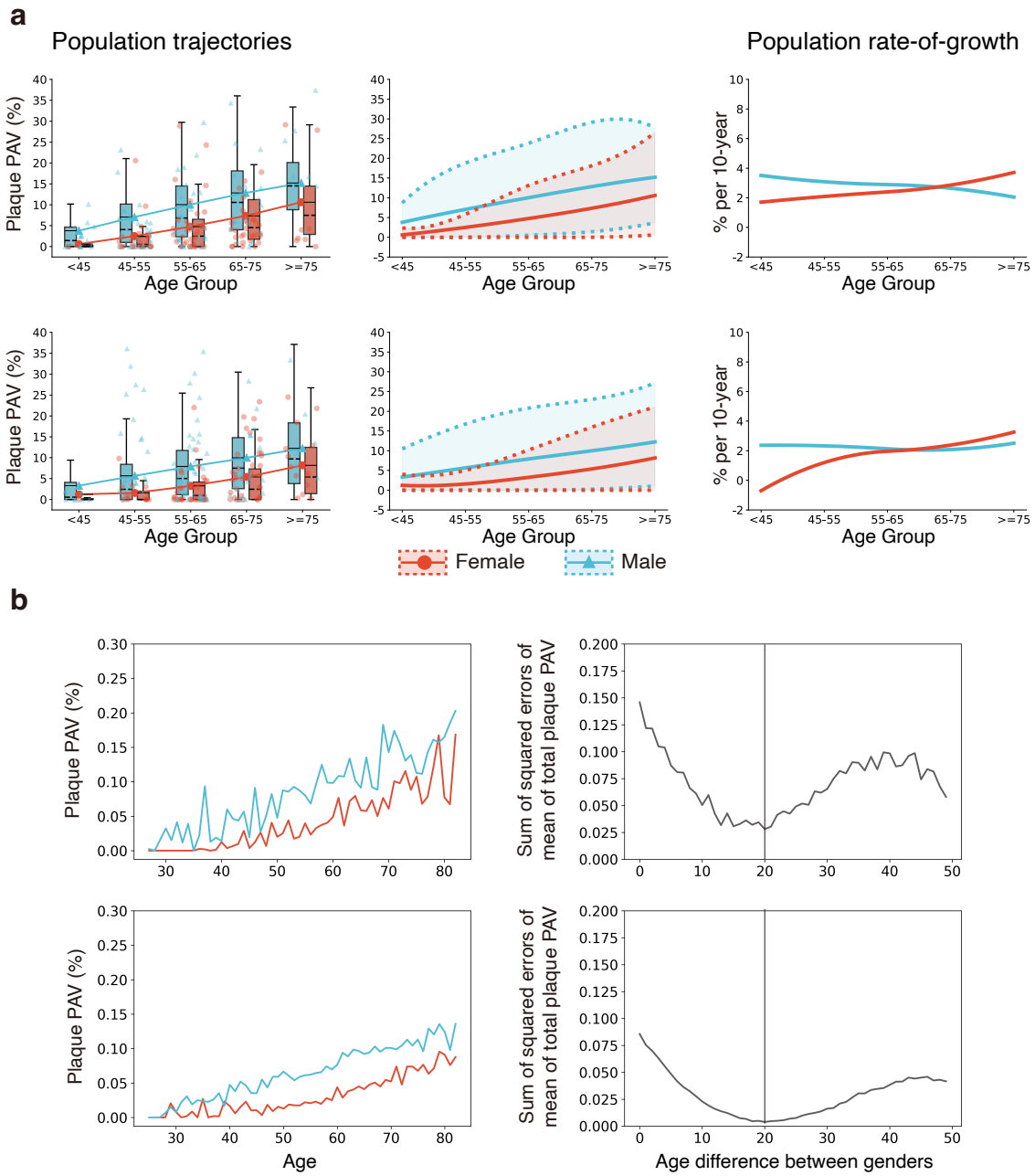

Supplementary Figure 3: **Sex differences in atherosclerosis onset and plaque progression between rural and urban populations. a,** Sex differences in plaque burden characteristics of rural (the 1st row) and urban (the 2nd row) populations. **b,** Disparities in atherosclerosis severity between sexes of rural (the 1st row) and urban (the 2nd row) populations.

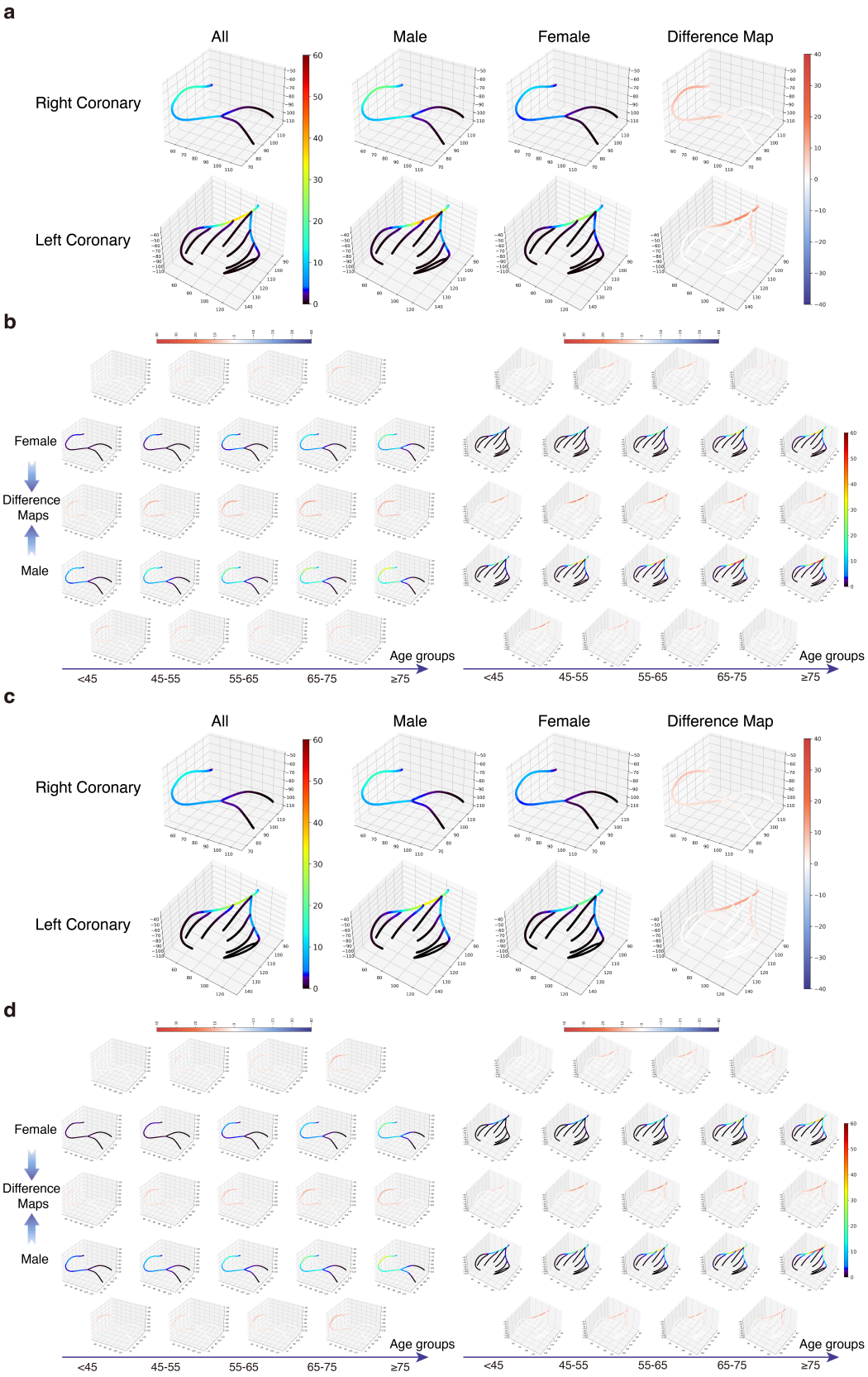

Supplementary Figure 4: **Spatiotemporal patterns of high-risk plaque and obstructive stenosis prevalence. a** and **c**, Spatial distribution of high-risk plaque (a) and obstructive stenosis (c) prevalence in all, male, and female groups of our cohort. The difference map is calculated by subtracting the male probability from the female probability at each position. **b** and **d**, Spatiotemporal distribution of high-risk plaque (b) and obstructive stenosis (d) prevalence by sex and age groups.

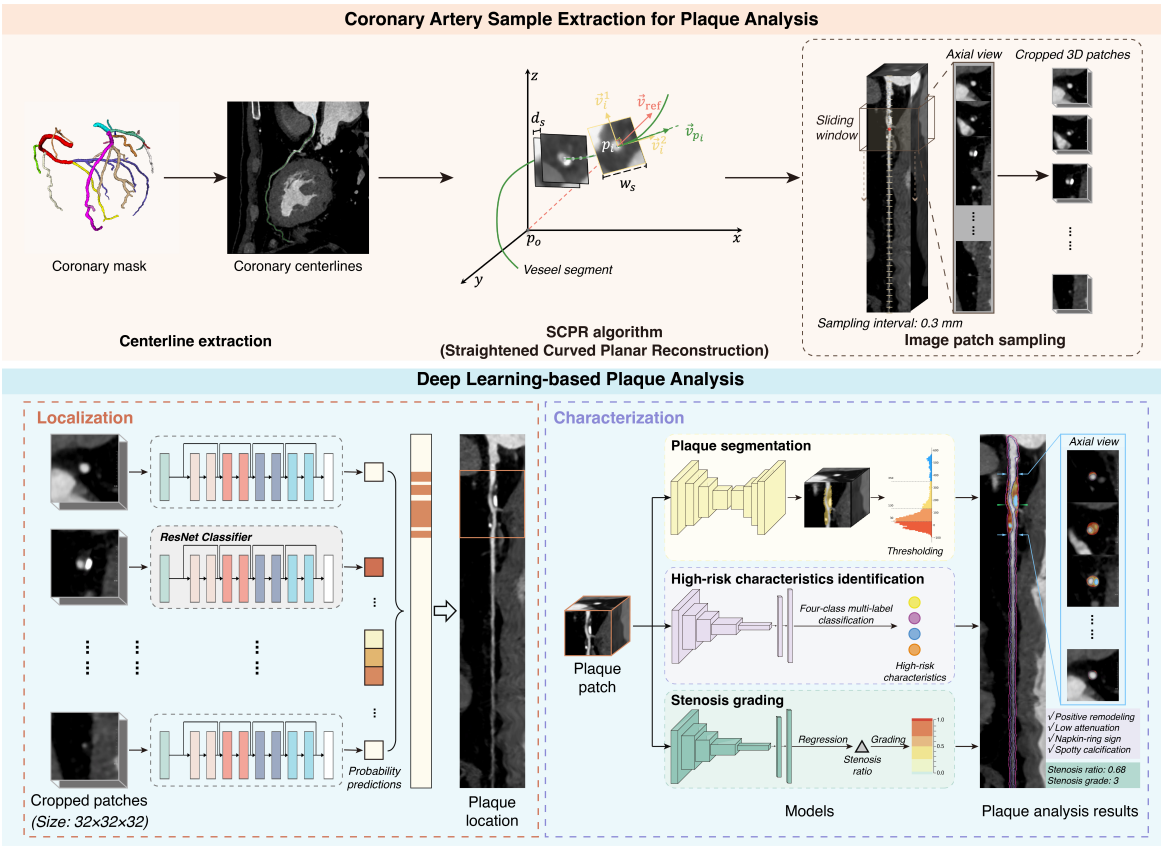

Supplementary Figure 5: Framework of the plaque detection, segmentation, high-risk feature classification and stenosis grading networks.

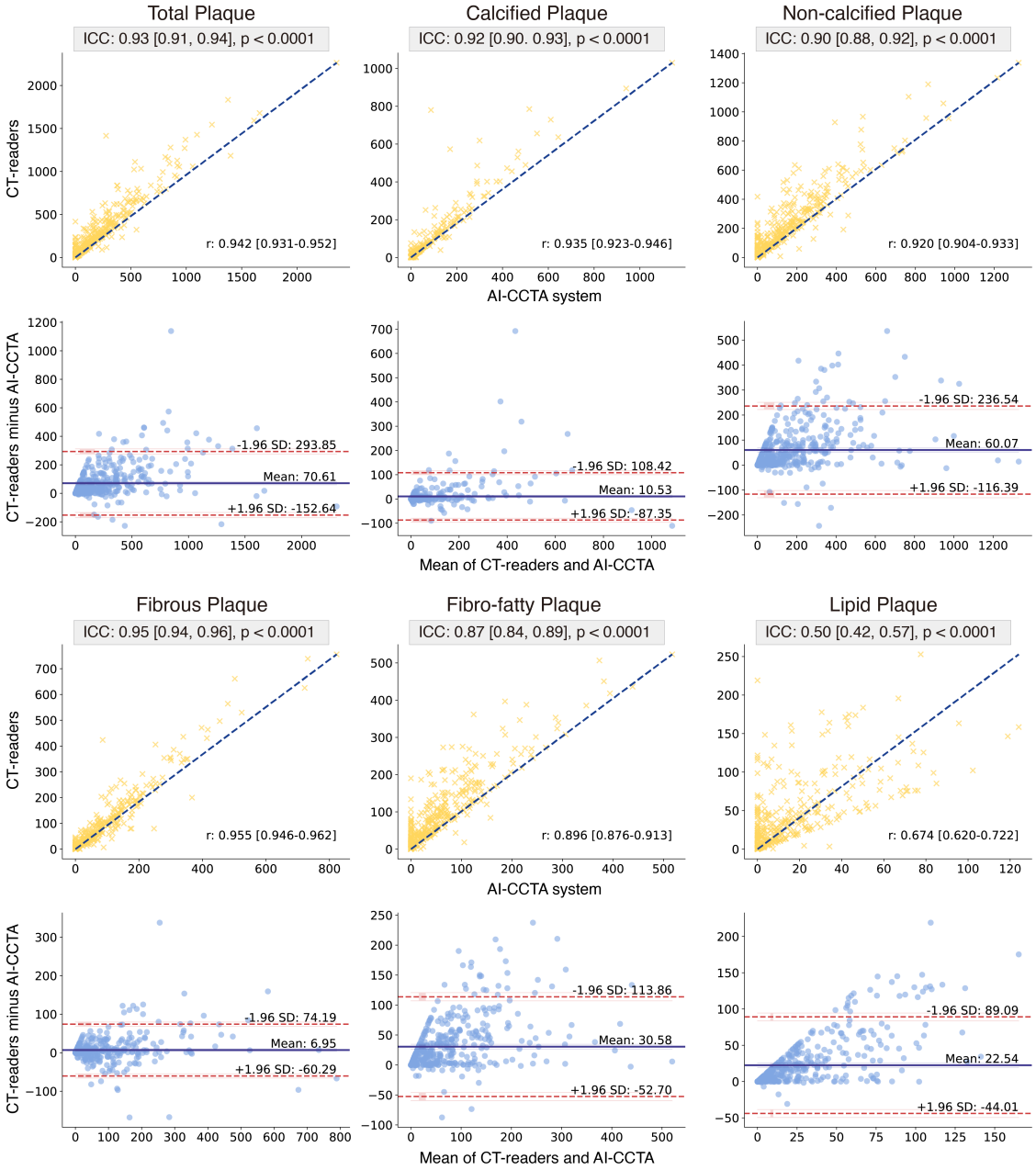

Supplementary Figure 6: **External validation of PLASMA against CT readers for plaque volume measurements** (n = 439)**.** Scatter plots (1st and 3rd rows) show Pearson's correlation coefficients, while Bland–Altman plots (2nd and 4th rows) illustrate the agreement between PLASMA and expert CT readers across six plaque types: total, calcified, non-calcified, fibrous, fibro-fatty, and lipid. Intraclass correlation coefficients (ICC), along with their 95% confidence intervals and significance values, are displayed in light gray boxes. ICC: intraclass correlation coefficient; SD: standard deviation.

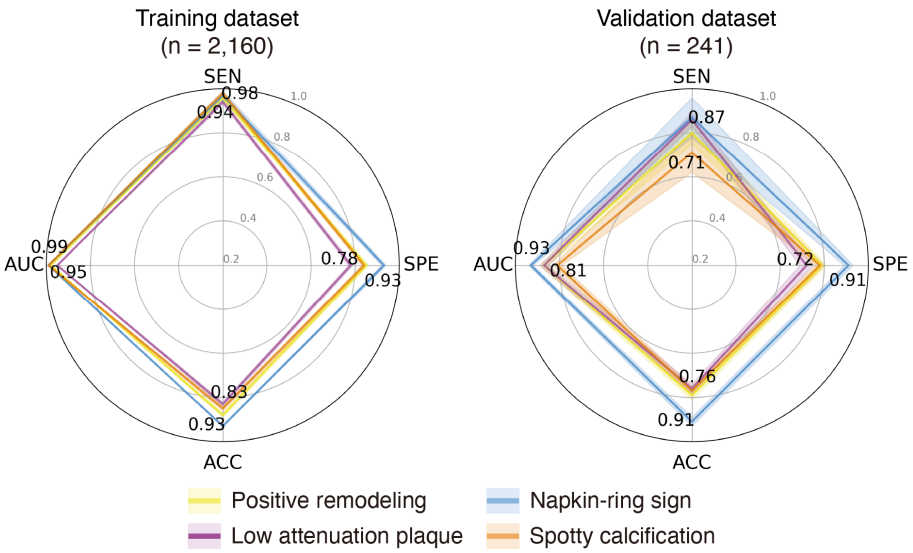

Supplementary Figure 7: **Evaluation of the PLASMA on high-risk plaque identification.** Radar plots showing the sensitivity (SEN), specificity (SPE), accuracy (ACC), and area under the curve (AUC) for four high-risk characteristics — positive remodeling (PR), low attenuation plaque (LAP), napkin ring sign (NRS), and spotty calcification (SC) - in the training ($n = 2,160$) and validation datasets ($n = 241$). Here, n represent the number of subjects in the dataset. Each characteristic is represented by a different color line, and the shaded regions indicate the 95% confidence intervals (CI).

Supplementary Table 3: Patient and plaque PAV characteristics.

	Entire Population	**Female**	**Male**	***p*-value**
Ours	16,300	6,780	9,520	
Tzimas G et.al. *	11,808	5,423	6,385	
Age, y †				
Ours	61.49±11.68 (25-97)	63.47±10.69 (26-96)	60.07±12.15 (25-97)	
Tzimas G et.al. *	62.7±12.2 (18-101)	63.4±12.5 (18-101)	62.0±11.9 (18-95)	
TP-PAV, % #				
Ours	6.60±8.42 3.28 (0.12-9.68)	4.47±6.74 1.56 (0-5.95)	8.11±9.14 4.99 (0.95-12.23)	1.16×10^{-166}
Tzimas G et.al. *	14.0±14.7 9.1 (1.2-22.8)	11.2±13.6 5.4 (0.5-18.0)	16.3±15.2 12.6 (2.8-26.4)	<0.0001
CP-PAV, % #				
Ours	1.87±3.56 0.27 (0-2.04)	1.43±3.03 0.08 (0-1.37)	2.18±3.87 0.45 (0-2.50)	2.88×10^{-39}
Tzimas G et.al. *	3.0±4.2 1.2 (0-4.5)	2.4±3.7 0.6 (0-3.3)	3.6±4.5 1.9 (0.2-5.4)	<0.0001
NCP-PAV, % #				
Ours	4.73±5.92 2.52 (0.04-7.06)	3.04±4.48 1.19 (0-4.30)	5.94±6.49 3.85 (0.75-8.97)	8.09×10^{-215}
Tzimas G et.al. *	10.9±11.0 7.6 (1.1-18.0)	8.8±10.3 4.6 (0.5-14.4)	12.7±11.3 10.3 (2.5-20.5)	<0.0001
FP-PAV, % #				
Ours	2.20±2.92 1.01 (0.01-3.18)	1.53±2.38 0.53 (0-2.01)	2.67±3.17 1.56 (0.26-3.98)	5.24×10^{-137}
Tzimas G et.al. *				
FFP-PAV, % #				
Ours	1.97±2.67 0.98 (0-2.81)	1.19±1.88 0.42 (0-1.63)	2.54±2.99 1.57 (0.27-3.71)	5.58×10^{-229}
Tzimas G et.al. *				
LP-PAV, % #				
Ours	0.56±0.94 0.18 (0-0.71)	0.33±0.64 0.05 (0-0.36)	0.73±1.08 0.32 (0.02-1.01)	8.08×10^{-163}
Tzimas G et.al. *	0.3±0.4 0.2 (0-0.5)	0.2±0.4 0.1 (0-0.4)	0.4±0.4 0.3 (0.1-0.6)	<0.0001

†Data are means±SDs and range (minimum-maximum).
#Data are means±SDs and median (IQR).
*Data are quoted from the comparative study of the North American population. Cells filled with diagonal lines represent missing data due to the lack of relevant information.
p values from Student's t test (two-sided) comparison. *p* values for Tzimas G et al. are reported as provided in the original publication. Adjustment for multiple comparisons was not performed.
TP = total plaque; CP = calcified plaque; NCP = non-calcified plaque; FP = fibrous plaque; FFP = fibro-fatty plaque; LP = lipid plaque; PAV = percent atheroma volume; SD = standard deviation; IQR = interquartile range.

Supplementary Table 4: Plaque volume characteristics stratified by rural and urban populations.

	Entire Population	**Female**	**Male**	***p*-value**
Rural	1377	639	738	
Urban	14923	6141	8782	
Age, y †				
Rural	58.12±11.54 (27-95)	60.53±10.50 (27-95)	56.04±11.99 (27-94)	
Urban	61.80±11.65 (25-97)	63.78±10.66 (26-96)	60.41±12.10 (25-97)	
TP-V, mm^3 #				
Rural	343.88±468.24 165.33 (24.76-469.94)	225.91±337.36 92.27 (0.00-310.35)	446.02±536.95 243.88 (69.53-646.31)	1.17×10^{-18}
Urban	291.78±415.65 126.16 (0.00-404.29)	177.21±295.72 53.10 (0.00-224.18)	371.90±465.65 207.69 (36.26-535.85)	3.48×10^{-179}
CP-V, mm^3 #				
Rural	73.86±161.74 5.99 (0.00-69.32)	54.03±118.52 1.76 (0.00-48.24)	91.02±189.85 13.84 (0.00-92.75)	2.19×10^{-05}
Urban	82.94±165.97 11.26 (0.00-86.30)	58.29±129.53 3.13 (0.00-52.73)	100.17±185.35 19.53 (0.00-112.93)	2.30×10^{-52}
NCP-V, mm^3 #				
Rural	270.02±353.81 137.67 (21.54-373.42)	171.88±245.12 80.92 (0.00-234.50)	355.00±407.57 222.07 (65.68-504.91)	2.07×10^{-22}
Urban	208.84±295.60 94.53 (0.00-287.95)	118.92±197.98 39.96 (0.00-156.21)	271.73±333.87 158.89 (28.83-387.58)	4.09×10^{-219}
FP-V, mm^3 #				
Rural	118.28±174.19 48.65 (4.88-160.18)	81.93±130.49 31.14 (0.00-100.10)	149.75±199.44 70.53 (17.56-210.20)	3.56×10^{-13}
Urban	98.42±150.11 39.18 (0.00-132.73)	61.06±107.63 17.97 (0.00-74.19)	124.55±168.92 63.66 (10.09-170.46)	9.24×10^{-146}
FFP-V, mm^3 #				
Rural	123.91±169.19 65.28 (9.40-169.91)	74.21±106.32 35.98 (0.00-98.37)	166.94±199.15 105.75 (31.93-237.17)	4.89×10^{-25}
Urban	86.03±129.69 36.34 (0.00-115.30)	45.35±80.23 13.45 (0.00-58.32)	114.48±148.71 63.64 (9.79-158.06)	2.79×10^{-233}
LP-V, mm^3 #				
Rural	27.83±47.70 10.34 (0.22-35.40)	15.74±26.98 4.02 (0.00-19.60)	38.30±58.14 18.40 (2.72-51.01)	7.06×10^{-19}
Urban	24.39±43.08 6.95 (0.00-30.10)	12.51±26.22 1.52 (0.00-13.31)	32.70±50.05 13.71 (0.67-43.67)	1.96×10^{-179}

†Data are means±SDs and range (minimum-maximum).
#Data are means±SDs and median (IQR).
p values were calculated using two-sided t-tests. Adjustment for multiple comparisons was not performed.
TP = total plaque; CP = calcified plaque; NCP = non-calcified plaque; FP = fibrous plaque; FFP = fibro-fatty plaque; LP = lipid plaque; V = volume; SD = standard deviation; IQR = interquartile range.

Supplementary Table 5: Subgroup analyses across seven major geographical regions in China.

	Entire Population	Female	Male
Sample Size			
East	3333	1461	1872
North	2680	1111	1569
Northeast	2979	1289	1690
Northwest	1120	434	686
Southwest	2100	841	1259
Central	2696	1071	1625
South	1392	573	819
Age, y †			
East	61.71±11.85 (27-96)	63.87±10.94 (28-95)	60.03±12.25 (27-96)
North	60.23±11.18 (26-91)	62.63±10.19 (27-90)	58.53±11.54 (26-91)
Northeast	59.42±11.70 (25-96)	61.17±10.73 (27-94)	58.10±12.22 (25-96)
Northwest	62.31±11.71 (25-97)	64.57±9.94 (31-94)	60.88±12.50 (25-97)
Southwest	62.79±11.52 (28-94)	64.69±10.56 (28-94)	61.52±11.95 (28-94)
Central	62.52±11.63 (25-96)	64.43±10.62 (26-96)	61.27±12.09 (25-93)
South	63.16±11.70 (27-94)	64.88±10.88 (27-94)	61.95±12.11 (28-93)
Total Plaque Volume, mm^3 #			
East	290.43±418.51	191.44±309.85	367.70±472.63
	131.46 (9.88–393.99)	71.49 (0.00–243.14)	195.49 (42.20–525.05)
North	375.45±482.78	232.61±357.61	476.59±531.98
	199.13 (22.49–545.53)	83.45 (0.00–293.02)	307.13 (76.44–684.98)
Northeast	260.50±398.51	147.01±262.37	347.07±458.46
	95.62 (0.00–348.25)	38.14 (0.00–177.11)	168.48 (16.31–493.37)
Northwest	303.97±414.76	200.97±324.64	369.13±451.02
	142.85 (16.83–425.32)	69.21 (0.00–249.87)	214.93 (40.39–540.76)
Southwest	255.27±376.37	146.59±239.12	327.86±430.13
	111.54 (0.00–357.93)	42.49 (0.00–193.86)	184.46 (29.70–469.77)
Central	296.16±419.91	181.48±296.67	371.74±469.29
	126.38 (3.89–414.97)	53.22 (0.00–233.99)	203.96 (34.57–525.55)
South	289.20±391.00	174.71±285.10	369.30±433.05
	132.48 (9.67–413.59)	51.67 (0.00–225.68)	218.64 (49.88–559.47)
Delayed Years, y			
East		18	
North		21	
Northeast		19	
Northwest		20	
Southwest		24	
Central		20	
South		25	

†Data are means±SDs and range (minimum-maximum).
#Data are means±SDs and median (IQR).
SD = standard deviation; IQR = interquartile range.